Evidence of bulk photovoltaic effect and large tensor coefficient in ferroelectric $BiFeO_3$ thin films

Wei Ji,[1,2] Kui Yao,[1,*] and Yung C. Liang[2]

[1]*Institute of Materials Research and Engineering (IMRE), A*STAR (Agency for Science, Technology and Research), 3 Research Link, Singapore 117602*

[2]*Department of Electrical and Computer Engineering, National University of Singapore, Kent Ridge, Singapore 119260*

(Received 1 July 2011; revised manuscript received 31 August 2011; published 23 September 2011)

We present a study on the bulk photovoltaic effect (BPVE) in ferroelectric thin films, in which the photocurrent is measured with symmetric electrodes in the plane perpendicular to the ferroelectric polarization to eliminate the effect of the depolarization field and interfacial energy barriers. We show evidence of a strong BPVE in epitaxial $BiFeO_3$ (BFO) films as thin as 40 nm. By taking into account the nonuniform absorption of incident photons, we obtain the bulk photovoltaic tensor coefficient β_{22} for BFO thin films. Remarkably, it is about five orders of magnitude larger than that of other typical ferroelectric materials for visible wavelengths. The results indicate that the BPVE in ferroelectric BFO thin films could be further explored for solar light photovoltaic applications.

DOI: 10.1103/PhysRevB.84.094115 PACS number(s): 73.50.Pz, 77.84.−s, 85.40.Xx, 77.55.Nv

I. INTRODUCTION

Recently the photovoltaic effect in ferroelectric thin films has attracted considerable interest. The photovoltaic effect can originate from a variety of mechanisms, such as the built-in electric field in a *p-n* junction,[1] a gradient in a chemical potential,[2] or spin polarization.[3] Another mechanism was discovered in noncentrosymmetric materials, such as ferroelectrics and is called the bulk photovoltaic effect (BPVE).[4] Ferroelectric materials have a unique spontaneous electrically polar direction, which can be switched by an external electric field. The asymmetry along this polar axis gives rise to the BPVE, which has been observed in both single crystals[5] and ceramics.[6] Unlike the photovoltaic effect observed in a *p-n* junction, BPVE does not require an asymmetric interface and its photovoltage is not limited by the band gap of the material.[7] However, applications based on the BPVE have so far been limited by its low efficiency.[4] Over the last few years, considerable progress has been seen on photovoltaics in ferroelectric thin films. It has been proposed that the efficiency can be improved in ferroelectric films with reduced thickness.[8] This has been demonstrated to a certain extent in (Pb,La)(Zr,Ti)O_3 (PLZT) thin films.[9] An open-circuit voltage much larger than the band gap has been observed in ferroelectric PLZT thin films with in-plane interdigitated electrodes[10] and ultraviolet (UV) sensors and dosimeters have been developed using ferroelectric thin films.[11] However, it should be highlighted that only the photocurrent along the polarization direction in PLZT films has been measured and reported in all these studies.

$BiFeO_3$ (BFO) is a ferroelectric and antiferromagnetic material at room temperature[12] with a band gap near 2.74 eV.[13,14] Recently we reported the photovoltaic effect in BFO thin films under visible light illumination, with a photocurrent switchable with respect to the direction of the ferroelectric polarization.[14] A switchable photocurrent strongly affected by the interfaces with electrodes was observed by Choi *et al.* in a BFO bulk single crystal.[15] It was also reported that the photovoltaic current in some BFO thin film samples cannot be switched at all and is entirely attributed to the interface depletion layer between the BFO and electrode.[16] Yang *et al.* demonstrated the photovoltaic effect in BFO films that arises from domain walls.[17] Some results in the reports from Choi *et al.*[15] and Kundys *et al.*[18] showed an angular dependence of the photocurrent on the light polarization direction, although this has never been interpreted as any BPVE. It should be highlighted that, in all the studies above on BFO and PLZT, only the photocurrent in the ferroelectric polarization direction has been studied, which makes it difficult to separate the effects of interfacial barriers and the depolarization field from the BPVE. As a result, none of the earlier studies can give insight to if and how BPVE contributes to the photovoltaic effect in ferroelectric thin films. In order to answer these questions, it is necessary to investigate the photocurrent in the plane perpendicular to the ferroelectric polarization (i.e., perpendicular to the depolarization field) with symmetric electrodes to clearly separate it from the significant effects of the interfacial energy barriers and the depolarization field.

BFO has the crystallographic point group of C_{3v} and belongs to the trigonal system. Its photovoltaic tensor should have a nonzero G_{22} component. A photocurrent should exist in the direction perpendicular to the ferroelectric polarization.[19] We prepared epitaxial BFO thin films directly on (111) $SrTiO_3$ (STO) substrates and measured the photocurrent in the direction perpendicular to the polarization direction under linearly polarized light. By investigating the angular dependence of this current on the incident light polarization, we show that BPVE exists in epitaxial BFO film as thin as 40 nm and that the photovoltaic tensor coefficient β_{22} of BFO is about five orders of magnitude larger than other typical ferroelectric materials for visible wavelengths.

II. DEVICE PREPARATION AND CHARACTERIZATION

A trigonal system can be described by either a rhombohedral or, as adopted in this report, a hexagonal unit cell.[20] BFO can also be indexed in the pseudocubic lattice. We use the subscripts "h" and "pc" to denote hexagonal and pseudocubic lattice, respectively. The relationship between the trigonal, rhombohedral, and pseudocubic unit cells is illustrated in Fig. 1(a). The coordinate transformation between the hexagonal and pseudocubic cells is given in the Appendix A.

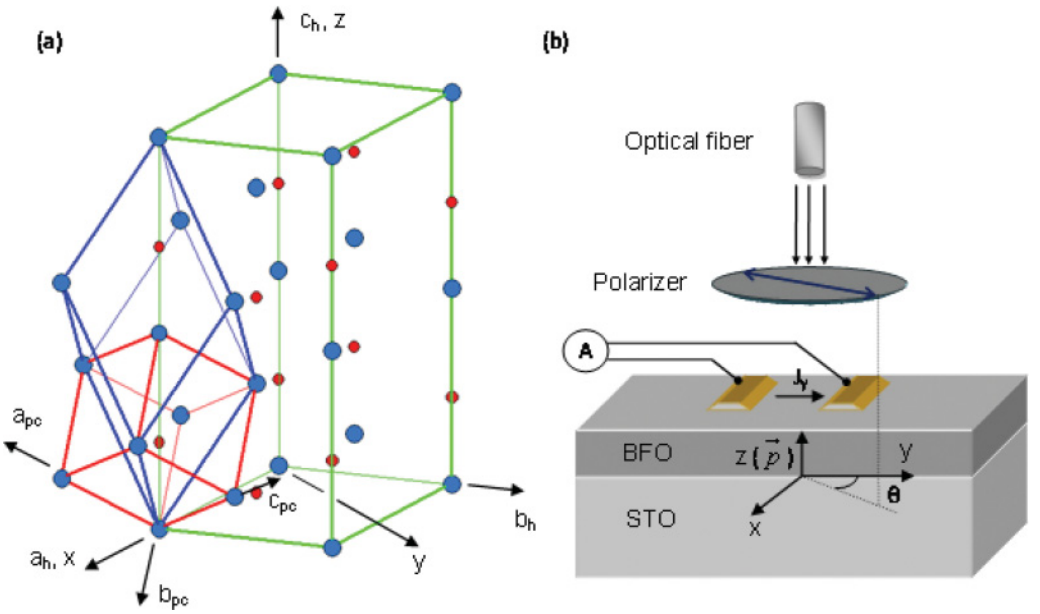

FIG. 1. (Color online) (a) Relationship between conventional hexagonal (green), rhombohedral (blue), and pseudocubic (red) unit cells for BFO and the Cartesian coordinates. Large blue sphere is Bi atom. Small red sphere is Fe atom. Oxygen atoms are omitted for clarity. (b) Schematic of the epitaxial BFO thin film with in-plane electrodes and polarization along thickness direction under polarized light. The angle between the polarizer transmission axis and the y axis is θ.

In order to calculate the BPVE tensor properties, one has to work in the Cartesian frame rather than in the crystallographic hexagonal frame. The z axis of the Cartesian coordinates coincides with the c axis of the hexagonal cell and is in the same direction as the ferroelectric polarization. The samples from our rf magnetron sputtering are self-polarized with the polarization direction pointing out of the film surface,[14] and this gives the direction of the z axis here. The x axis of the Cartesian coordinates coincides with the crystallographic axis **a** ($[100]_h$) in the hexagonal cell.[21] The y axis is perpendicular to both the z and x axes, forming a right-hand coordinate system, as shown in Fig. 1(b).

BFO thin films were prepared by rf magnetron sputtering using a ceramic target with composition of $Bi_{1.1}FeO_3$. The deposition was carried out at 600 °C, with an Ar:O_2 ratio of 11:1 and a working pressure of 12 mTorr. Au in-plane electrodes with a gap of 0.14 mm were patterned by a standard photolithography process [Fig. 1(b)].

The short-circuit photocurrent was measured with an electrometer (Keithley 6517A) with an incident light of 435 nm.[14] The light propagated perpendicular to the sample surface and the incident intensity was 20 mW/cm^2. A Glan-Taylor polarizer was used to rotate the light polarization in the $(001)_h$ plane. After the polarizer angle was adjusted, the short-circuit photocurrent was measured and the steady-state readings were used for the calculation [Fig. 3(a) inset].

Reciprocal space mapping (RSM) by high resolution x-ray diffraction (HRXRD) shows that the BFO films grow epitaxially on the (111) STO substrates with a rhombohedral structure for all samples (Fig. 2).[22] The interplanar spacings of $(006)_h$ and $(024)_h$ are $d_{(006)} = 2.312$ Å and $d_{(024)} = 1.985$ Å, respectively, for 466-nm-thick film, and $d_{(006)} = 2.312$ Å and $d_{(024)} = 1.984$ Å, respectively, for 40-nm-thick film. They are almost the same as the values reported for bulk BFO.[20] The in-plane orientation of the BFO films was determined by x-ray diffraction (XRD) azimuthal phi scans. The (200) planes of the substrate and the $(200)_{pc}$ of BFO films were found to coincide with each other. This was used to determine the y axis of the Cartesian coordinates. The projection of $[001]_{pc}$ in the $(001)_h$ plane is the y axis of the hexagonal lattice (Appendix A). Atomic force microscopy (AFM) measurements show a uniform morphology of the film surfaces. The roughness for the thinnest 40-nm-thick film is about 3.57 nm.

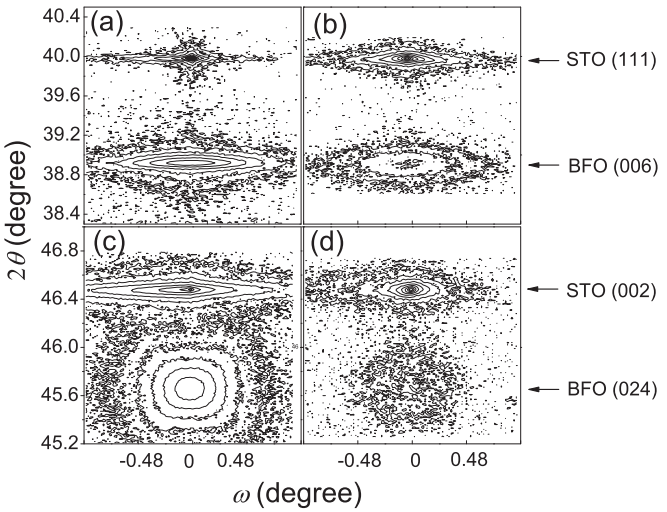

FIG. 2. RSM of epitaxial BFO thin films on STO substrates. (a) (111) 446 nm film; (b) (111) 40 nm film; (c) (002) 446 nm film; (d) (002) 40 nm film.

III. TENSORIAL PHOTOCURRENT IN THIN FILMS

Repeatable continuous photocurrent was obtained when the samples were illuminated [Fig. 3(a) inset]. The short-circuit current densities at different polarizer angles for the samples with six different thicknesses are presented in Fig. 3(a). Since the magnitude of the photocurrent varied with sample thickness, the results for individual samples were normalized. The current density was also slightly affected by the minor variation in light intensity when the polarizer was rotated. To minimize the effect of such minor variations in our analysis, the average of the normalized current density for all the samples was calculated. The result was fitted very well to a cosine function, as shown in Fig. 3(b). The fitting function is

$$J_y = 0.801 \cos\left[2.087\,(\theta + 0.154)\right]. \tag{1}$$

Equation (1) shows an offset of about 8.8° from origin, caused mainly by the misalignment of the crystal axes, the in-plane electrodes, and the incident light polarization direction.

It should be emphasized that the photocurrent measured here is perpendicular to the ferroelectric polarization. Therefore, our results cannot be explained by the depolarization field.[8,14,15] This, and the low incident intensity employed here, rule out second-order optical effects as well.[23] The use of symmetric in-plane electrodes also exclude the photovoltaic effect from asymmetric energy barriers.[24] Other proposed mechanisms, such as the electrostatic potential at domain walls,[17] cannot explain the angular dependence of the photocurrent here. Such an angular dependence can be described in the framework of the bulk photovoltaic theory, where the photocurrent is produced as a consequence of asymmetric microscopic processes such as excitation and recombination.[4] According to this theory, the dependence of the photocurrent on the incident light polarization can be expressed by a bulk photovoltaic tensor. As BFO has a high absorption coefficient at the incident wavelength,[14] it is necessary here to modify the formulas by explicitly expressing the light intensity as a function of film thickness (Appendix B). The result for the current density in the y-axis direction is

$$\begin{aligned} J_y &= I(0) G_{22} \frac{1 - \exp(-\alpha d)}{d} \cos 2\theta \\ &= I(0) \beta_{22} \frac{1 - \exp(-\alpha d)}{\alpha d} \cos 2\theta, \end{aligned} \tag{2}$$

where $I(0)$, G, β, α, and d are the incident intensity, Glass constant, tensor coefficient, absorption coefficient, and film thickness, respectively (Appendix B). Equation (2) describes the current along the y direction as a cosine function of 2θ, in which θ is the angle between the light polarization and the y axis. This is in agreement with the experimental result shown in Fig. 3, as described in Eq. (1).

The photocurrent density increases with decrease in film thickness, as shown in Fig. 4. By fitting our results to Eq. (2), we can obtain the values of α, G_{22}, and β_{22}. The Glass coefficient G_{22} is 4.48×10^{-10} cm/V, comparable to other ferroelectric materials.[4] The absorption coefficient α is found to be 2.5×10^5 cm^{-1}. The strong absorption may be a consequence of absorption at the direct band gap of BFO. The tensor coefficient β_{22} is around 1.1×10^{-4} V^{-1}, which is about five orders of magnitude larger than typical values for both $LiNbO_3$:Fe and $LiTaO_3$ (Ref. 4), which belong to the same C_{3v} point group as BFO and is six orders of magnitude larger than that of PLZT.[25] The significantly larger β_{22} for BFO can be attributed to the much large absorption coefficient α. Our BFO samples displayed a high resistivity on the order of 10^{12} Ω cm at low field, similar to our previous report.[14] This rules out the possible enhancement of the photocurrent due to a small internal resistance.[15]

From the theoretical analysis, it is difficult to conclusively determine the direction of the BPVE photocurrent along the z axis because of the unknown sign of G_{31}. However, our experimental photovoltaic results for epitaxial BFO films on $SrRuO_3$-buffered (001) and (111) STO substrates with indium-tin-oxide (ITO) top electrodes provide clues about this issue. The polarization vector in these films pointed to the top electrode.[14] The experimentally observed photocurrent traveled from the top electrode to the bottom electrode inside the films; i.e., in the direction of the depolarization field.[26] What is interesting is that the current density was two orders of magnitude larger in the (001) film than in (111) film (Fig. 5).

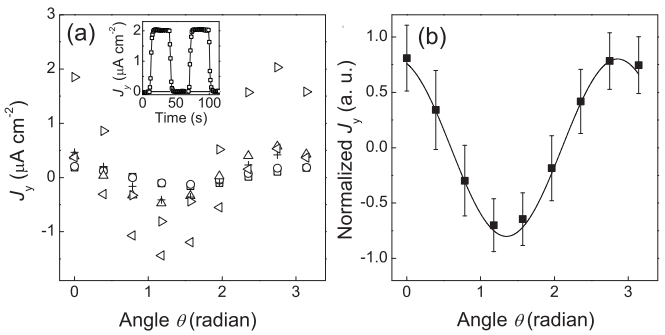

FIG. 3. Short-circuit photocurrent density J_y. (a) J_y of samples with different thicknesses, (□) 446 nm, (○) 335 nm, (△) 223 nm, (+) 135 nm, (◁) 80 nm, (▷) 40 nm. Inset shows time dependence of J_y. (b) Normalized J_y at different polarizer angles. The error bar is one standard deviation of the readings from different samples.

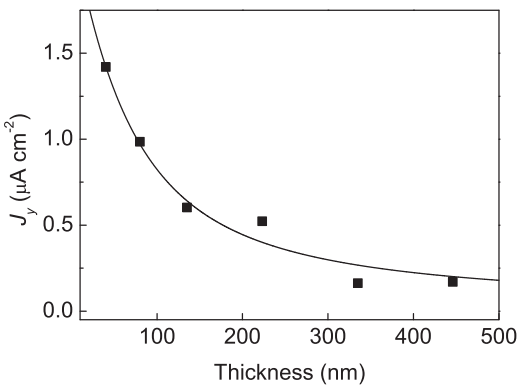

FIG. 4. BPVE current density J_y for samples with different thicknesses. Solid line shows curve fit from Eq. (2).

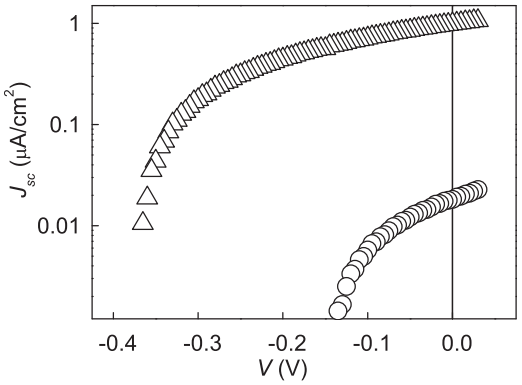

FIG. 5. Short-circuit photocurrent density along surface normal direction in a (111) BFO film (○) and a (001) BFO film (△) at the same light intensity of 5.8 mW/cm^2, both with $SrRuO_3$ and ITO as the bottom and top electrode, respectively.

This can be well explained if the BPVE current was assumed to be opposite to the depolarization field. The magnitude of the BPVE tensor coefficient β_{31} and β_{33} is usually one order of magnitude larger than β_{22} (Ref. 4), and here can be estimated to be on the order of 1×10^{-3} V^{-1}. Thus the estimated magnitude of the BPVE photocurrent density along the z axis is on the order of μA/cm^2 at the intensity of 5.8 mW/cm^2, which is comparable to the magnitude of photocurrent as observed in the (001) films. The two current components originating from the depolarization field and the BPVE had similar magnitude and, thus, only a very small current could be detected in the case of the (111) BFO films. However, as the polarization vector of (001) BFO forms an angle of 54.7° with the surface normal, the BPVE photocurrent collected at the $(001)_{pc}$ face was reduced by about half, resulting in a much larger photocurrent in the direction opposite to the polarization (i.e., aligned with the depolarization field). Therefore, we thought that the BPVE current in BFO along the film thickness should flow in the same direction as the ferroelectric polarization, and opposite to the depolarization field. This means the photocurrent along the depolarization field direction as reported in BFO in the literature may be significantly cancelled by BPVE, and the understanding developed here may lead to designs that dramatically improve the photovoltaic response in ferroelectric thin films.

IV. CONCLUSION

By investigating photocurrent under polarized visible light in the plane of the surface in epitaxial $BiFeO_3$ (BFO) thin films with the polarization in the thickness direction, we observed the photocurrent in the plane perpendicular to the ferroelectric polarization (i.e., perpendicular to the depolarization field) with symmetric electrodes. Evidence of the strong bulk photovoltaic effect (BPVE) was obtained in epitaxial BFO films as thin as 40 nm. In addition, it was noted that the bulk photovoltaic tensor coefficient in BFO thin films is about five orders of magnitude larger than that of other typical ferroelectric materials for visible wavelengths. Therefore, the BPVE in ferroelectric BFO thin films could be further explored for solar light photovoltaic applications.

ACKNOWLEDGMENTS

The authors thank R. N. Premnath for discussions about the sputtering process. We acknowledge the research grant support from Institute of Materials Research and Engineering (IMRE), A-STAR, through project IMRE/10-1C0109 and acknowledge the facility supports at the central cleanroom of IMRE and SERC nano Fabrication, Processing and Characterisation (SnFPC) for sample fabrication.

APPENDIX A: COORDINATE TRANSFORMATION BETWEEN HEXAGONAL AND PSEUDOCUBIC LATTICE FRAMES

The relationship of the basis vectors between the hexagonal lattice frame and the pseudo-cubic lattice frame is

$$\mathbf{a}_{i,h} = \alpha_{ij}\mathbf{a}_{j,pc}; \tag{A1}$$

$$\mathbf{a}_{i,pc} = \alpha_{ij}^{-1}\mathbf{a}_{j,h}, \tag{A2}$$

with the transformation matrices expressed as

$$\alpha = \begin{pmatrix} 1 & 1 & 0 \\ -1 & 0 & 1 \\ 2 & -2 & 2 \end{pmatrix}, \tag{A3}$$

$$\alpha^{-1} = \frac{1}{3}\begin{pmatrix} 1 & -1 & \frac{1}{2} \\ 2 & 1 & -\frac{1}{2} \\ 1 & 2 & \frac{1}{2} \end{pmatrix}. \tag{A4}$$

It can be shown that the lattice vector $[110]_{pc}$ is equivalent to $[100]_h$ (x axis):

$$\mathbf{p}_{pc} = [100]_h \begin{pmatrix} 1 & 1 & 0 \\ -1 & 0 & 1 \\ 2 & -2 & 2 \end{pmatrix} = [110]_{pc}. \tag{A5}$$

Without considering the small distortion of the pseudocubic structure, the lattice direction $[001]_{pc}$ is perpendicular to $[110]_{pc}$:

$$[110]_{pc} \cdot [001]_{pc} = 0. \tag{A6}$$

Thus, the projection of $[001]_{pc}$ in the $(001)_h$ plane is the y axis of the hexagonal lattice.

APPENDIX B: DERIVATION OF BULK PHOTOVOLTAIC PHOTOCURRENT DENSITY IN THIN FILMS

The incident light that propagates along the z axis can be expressed as

$$\begin{aligned} \mathbf{E} &= |E|\{\mathbf{e}_x \sin(\theta)\exp[i(\mathrm{k_o z} - \omega \mathrm{t})] \\ &\quad + \mathbf{e}_y \cos(\theta)\exp[i(\mathrm{k_o z} - \omega \mathrm{t})]\} \\ &= |E|(\mathbf{e}_x e_1 + \mathbf{e}_y e_2). \end{aligned} \tag{B1}$$

For a sample with a weak absorption coefficient, uniform absorption can be assumed. The resultant photocurrent density can be calculated as

$$\mathbf{J} = I \begin{bmatrix} 0 & 0 & 0 & 0 & \beta_{15} & -\beta_{22} \\ -\beta_{22} & \beta_{22} & 0 & \beta_{15} & 0 & 0 \\ \beta_{31} & \beta_{31} & \beta_{33} & 0 & 0 & 0 \end{bmatrix} \begin{bmatrix} e_1^2 \\ e_2^2 \\ 0 \\ 0 \\ 0 \\ e_1 e_2^* \end{bmatrix}$$

$$= I \begin{bmatrix} -\beta_{22} e_1 e_2^* \\ -\beta_{22} e_1^2 + \beta_{22} e_2^2 \\ \beta_{31} e_1^2 + \beta_{31} e_2^2 \end{bmatrix} = I\alpha \begin{bmatrix} -G_{22} \sin\theta \cos\theta \\ -G_{22} \sin^2\theta + G_{22} \cos^2\theta \\ G_{31} \end{bmatrix}. \tag{B2}$$

The components of the photocurrent along the different axes are

$$J_x = -I\alpha G_{22} \sin\theta \cos\theta = -\tfrac{1}{2} I\alpha G_{22} \sin 2\theta, \tag{B3}$$

$$J_y = I\alpha G_{22}(-\cos^2\theta + \sin^2\theta) = I\alpha G_{22} \cos 2\theta, \tag{B4}$$

$$J_z = I\alpha G_{31}. \tag{B5}$$

In a medium with strong absorption, the photocurrent is mainly generated near the illuminated surface and becomes a function of penetration depth. As a result, the above equations need to be modified. Next, we consider explicitly the nonuniform absorption of light in thin films. For clarity, we first derive J_y when the light polarization coincides with the y axis ($\theta = 0$). We denote the parameters as follows:

(i) s: length of electrode,
(ii) l: electrode gap,
(iii) d: film thickness,
(iv) $I(x)$: incident intensity at the depth of x.

The current density by absorption in a differential volume $dxdydz$ is

$$J_y = \alpha G_{22} I = \alpha G_{22} I(0) \exp(-\alpha z). \tag{B6}$$

The current through a differential area $dzdx$ is

$$T_y' = J_y dz dx = \alpha G_{22} I(0) \exp(-\alpha z)\, dz dx. \tag{B7}$$

The total current through the face sd is

$$T_y = \int_{0,0}^{z=d,x=s} J_y dz dx = \alpha G_{22} I(0) \int_{0,0}^{z=d,x=s} e^{-\alpha z} dz dx$$
$$= s G_{22} I(0)[1 - \exp(-\alpha d)]. \tag{B8}$$

The current density is

$$J_{y,\theta=0} = \frac{T}{sd} = G_{22} I(0) \frac{1 - \exp(-\alpha d)}{d}, \tag{B9}$$

where

$$G_{22} = \frac{\beta_{22}}{\alpha}. \tag{B10}$$

Similar expressions can be derived for the photocurrent in other directions. The current density with angular dependence along the y axis is

$$J_y = I(0) G_{22} \frac{1 - \exp(-\alpha d)}{d} \cos 2\theta$$
$$= I(0) \beta_{22} \frac{1 - \exp(-\alpha d)}{\alpha d} \cos 2\theta. \tag{B11}$$

*k-yao@imre.a-star.edu.sg

[1] J. Nelson, *The Physics of Solar Cells* (Imperial College Press, London, 2003).
[2] B. A. Gregg, J. Phys. Chem. B **107**, 4688 (2003).
[3] S. D. Ganichev and W. Prettl, J. Phys.: Condens. Matter **15**, R935 (2003).
[4] B. I. Sturman and V. M. Fridkin, *The Photovoltaic and Photorefractive Effects in Noncentrosymmetric Materials* (CRC Press, Boca Raton, 1992).
[5] G. Dalba, Y. Soldo, F. Rocca, V. M. Fridkin, and P. Sainctavit, Phys. Rev. Lett. **74**, 988 (1995).
[6] S.-Y. Chu, Z. Ye, and K. Uchino, Smart Mater. Struct. **3**, 114 (1994).
[7] A. M. Glass, D. von der Linde, and T. J. Negran, Appl. Phys. Lett. **25**, 233 (1974).
[8] M. Qin, K. Yao, and Y. C. Liang, App. Phys. Lett. **95**, 022912 (2009).
[9] M. Qin, K. Yao, and Y. C. Liang, Appl. Phys. Lett. **93**, 122904 (2008).
[10] K. Yao, B. K. Gan, M. Chen, and S. Shannigrahi, Appl. Phys. Lett. **87**, 212906 (2005).
[11] B. K. Gan, K. Yao, S. C. Lai, Y. F. Chen, and P. C. Goh, IEEE Electron Device Lett. **29**, 1215 (2008).
[12] G. Catalan and J. F. Scott, Adv. Mater. **21**, 1 (2009).
[13] J. F. Ihlefeld *et al.*, Appl. Phys. Lett. **92**, 142908 (2008).
[14] W. Ji, K. Yao, and Y. C. Liang, Adv. Mater. **22**, 1763 (2010).
[15] T. Choi, S. Lee, Y. J. Choi, V. Kiryukhin, and S. W. Cheong, Science **324**, 63 (2009).
[16] S. Y. Yang *et al.*, Appl. Phys. Lett. **95**, 062909 (2009).
[17] S. Y. Yang *et al.*, Nat. Nanotechnol. **5**, 143 (2010).
[18] B. Kundys, M. Viret, D. Colson, and D. O. Kundys, Nat. Mater. **9**, 803 (2010).
[19] V. M. Fridkin, Crystallography Reports **46**, 654 (2001).
[20] Powder diffraction data 2, PDF# 01-071-2494 (International Center for Diffraction Data, Newton, PA, 2008).
[21] R. E. Newnham, *Properties of Materials: Anistropy, Symmetry, Structure* (Oxford University Press, Oxford, 2005).
[22] S. E. Lofland, K. F. McDonald, C. J. Metting, and E. Knoesel, Phy. Rev. B **73**, 092408 (2006).
[23] K. Tonooka, P. Poosanaas, and K. Uchino, SPIE **3324**, 224 (1998).
[24] L. Pintilie and M. Alexe, J. Appl. Phys. **98**, 124103 (2005).
[25] M. Ichiki, H. Furue, T. Kobayashi, Y. Morikawa, K. Nonaka, T. Nakada, Z. J. Wang, and R. Maeda, Jpn. J. Appl. Phys. **45**, 9115 (2006).
[26] R. R. Mehta, B. D. Silverman, and J. T. Jacobs, J. Appl. Phys. **44**, 3379 (2003).